Effect of atmosphere on growth of single crystal zinc oxide nanowires

SEU YI LI, PANG LIN
Institute of Materials Science and Engineering, National Chiao Tung University, Hsinchu 30049, Taiwan, ROC

CHIA YING LEE, TSEUNG YUEN TSENG
Department of Electronics Engineering and Institute of Electronics, National Chiao Tung University, Hsinchu 30050, Taiwan, ROC
E-mail: tseng@cc.nctu.edu.tw

Single crystal zinc oxide (ZnO) nanowires were prepared by using enhanced two-step vapor–liquid–solid (VLS) growth mechanism. The experimental results indicate that the growth rate and morphologies of the nanowires depends on the carrier gas ambient during the thermal reaction process. The ZnO nanowire grown with N_2, not only has the smaller diameter of about $\sim$ 30 nm but also exhibits a higher growth rate and larger number of density of nanowires per unit area than those grown with Ar. The photoluminescence measurements show that the ZnO nanowires grown with N_2 have a stronger ultraviolet emission than those grown with Ar.

1. Introduction

One-dimensional (1D) nanostructures, e.g., carbon nanotubes, metal oxide nanobelts (ribbons), and nanowires of metals, oxides, and semiconductors, have drawn much attention because of their interesting growth mechanism, physical property, and lots of application in the electronic and optical nanodevices. Recently, much works have been performed with the unique characteristics of semiconductor nanowires. Optical explorations of epitaxially grown nanowires have focused on the giant emission in photoluminescence characteristics. Recent reports have shown that zinc oxide (ZnO) nanowires exhibit ultraviolet (UV) laser emission, which can be used in luminescent device applications [1–4]. A variety of methods such as the two-step vapor–liquid–solid (VLS) growth process [5], laser-assisted catalytic growth (LCG) method [6], chemical vapor deposition (CVD) [7], template [8] and other methods [9] have been employed to synthesize nanowires of different materials.

Among various preparation methods, the metal catalytic VLS growth process provides a cheap and speedy route for large-area deposition of nanowires. The physical structures of the nanowires are affected strongly by the fabricating parameters such as starting materials, temperature, time and atmosphere. However, the effect of atmosphere on the structure and property of ZnO nanowires was scarcely studied. In the present study, we grow ZnO nanowires on Si (1 0 0) p-type substrate by using Cu catalyzed VLS with Ar and N_2 carrying gases. The effects of atmosphere on the morphology, structure and optical property of those nanowires were studied.

2. Experimental

The Si (1 0 0) substrate was cleaned in an ultrasonic bath of acetone. The 70 Å thick catalytic copper thin films were deposited on cleaned Si (1 0 0) substrates by rf-sputtering. Equal amounts of ZnO powder and graphite powder obtained from Alfa Aesar were milled, loaded into an alumina boat and placed in the center of a quartz tube. The quartz tube was laid in a furnace, which was controlled to be at 850–950 °C. The N_2 and Ar were used as carrier gas. The ZnO nanowires were grown under flowing gas with the gas flow rate of 5 $\sim$ 40 sccm.

ZnO nanowires were synthesized by VLS growth mechanism under different carrier gases employed during the thermal process. After the carbothermal reaction, ZnO nanowires formed on the substrate and the colors of the products were grayish white and gray when N_2 and Ar were used as carrier gases, respectively. Significant growth of ZnO nanowires was detected immediately as the synthesis temperature, i.e., 850 $\sim$ 950 °C was attained. This observation implies that the nanowires grow rapidly once the nucleus form. The growth-limiting conditions depend on the supersaturate droplets, which catalyze the nanowires growth.

The crystal structure and composition of the nanowires were studied by X-ray diffraction (XRD, MAC Sience, MXP18, Japan), X-ray photoelectron spectroscopy (XPS, VG Scientific ESCALAB 250, England), Auger electron spectroscopy (AES, VG Scientific Microlab 350) and nanometer-scale energy-dispersive X-ray spectroscopy (EDX, JEOL-2010, Japan). The morphology and size distribution of the nanowires were characterized using field-emission scanning electron

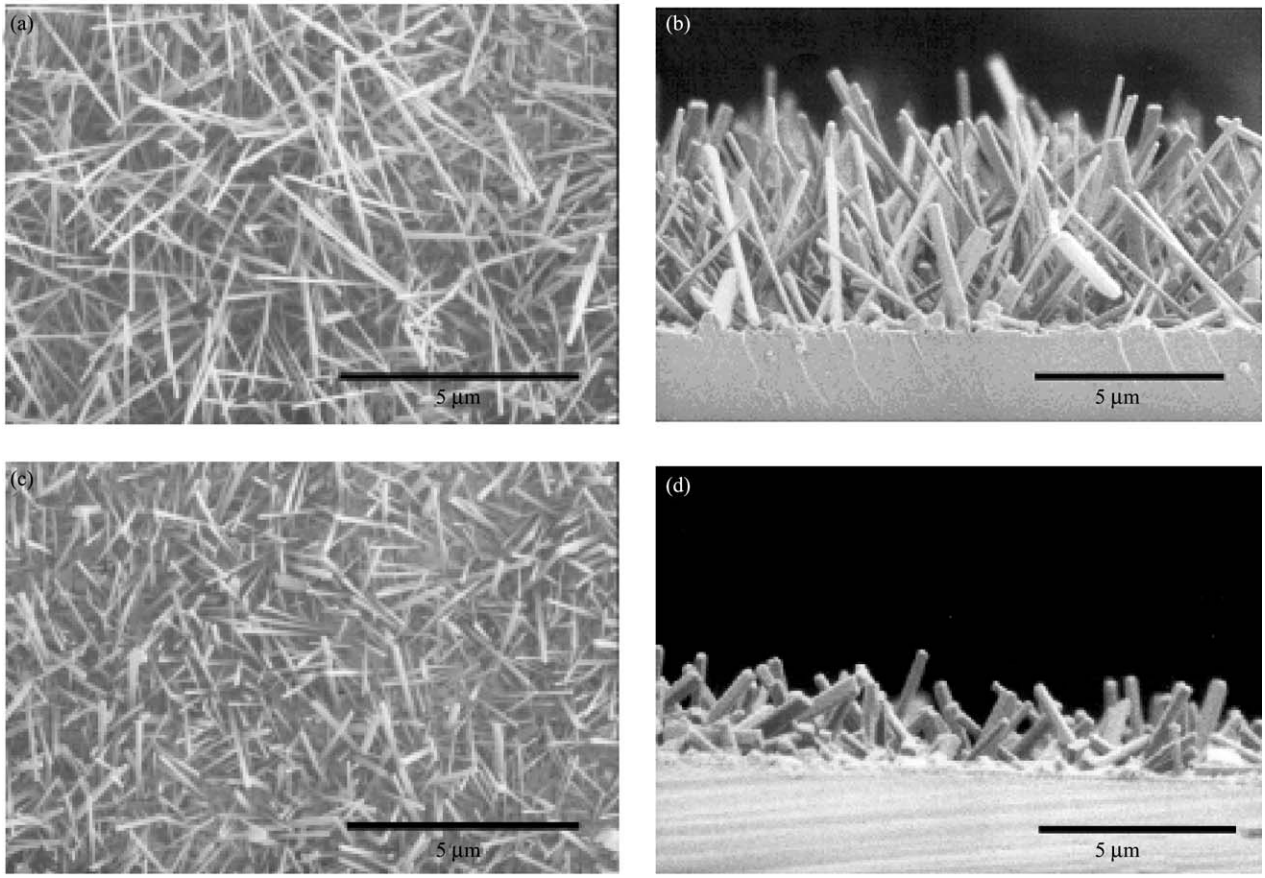

Figure 1 SEM images of the ZnO nanowires synthesized at 900 °C for 3 min. The nanowires shown in (a) and (b) were synthesized in N_2, while (c) and (d) in Ar.

microscopy (FESEM, Hitachi, S-4700I) and high resolution transmission electron microscopy (HRTEM, Philip, tecnai-20). A fluorescence spectrophotometer (PL, Hitachi, F-4500), with Xe lamp as excitation source, was used for the luminescence study of ZnO nanowires at room temperature.

3. Results and discussion

The typical FE-SEM morphologies of the ZnO nanowires are shown in Fig. 1. The number of density and dimensions of nanowires depend on kind of the carrier gas used during the VLS process. The images of the ZnO nanowires synthesized in N_2 gas after 12 min. Fig. 1(a) and (b) show the widths of nanowires ranged from $\sim$ 30 to $\sim$ 50 nm and length of about 5 μm, while those of Ar synthesized nanowires (Fig. 1(c) and (d)) are 70–100 nm and about 3 μm, respectively. Such geometrical difference maybe attributed to the difference in viscosities of Ar and N_2 ($\eta_{Ar} = 6.4 * 10^{-4}$ g/cm s and $\eta_{N_2} = 4.8 * 10^{-4}$ g/cm s at 900 °C [10]). The average growth rate of ZnO nanowires in N_2 is about 6.95 nm/s, whereas the average growth rate of those in Ar atmosphere is about 4.17 nm/s. Generally, the lower viscosities cause faster gas flow pattern, which is suitable for efficient zinc vapor transport on to the droplet surface of the catalyst that eventually speeds up the growth of ZnO nanowires. Cross-section SEM images (Fig. 1(b)) reveal that the nanowires grow almost perpendicular to the substrate surface without any buffer layer.

The variation in length of ZnO nanowires with growth time in different carrier gases, Ar and N_2, is shown in Fig. 2. It is observed that the diameters and the lengths of the nanowires increase with time during this process. The growth process approaches saturation point in about 12 min for both gases, as indicated in the Fig. 2. Beyond the saturation point, the diameter of the ZnO nanowires grown in both gases becomes wider and is about 70 nm. Moreover, the plot of the length vs. growth time of the ZnO nanowires grown in N_2 has a sharper slope than that in Ar. Therefore, the synthesis speed of ZnO nanowires in N_2 is faster than in Ar at the same growth temperature 850 $\sim$ 950 °C.

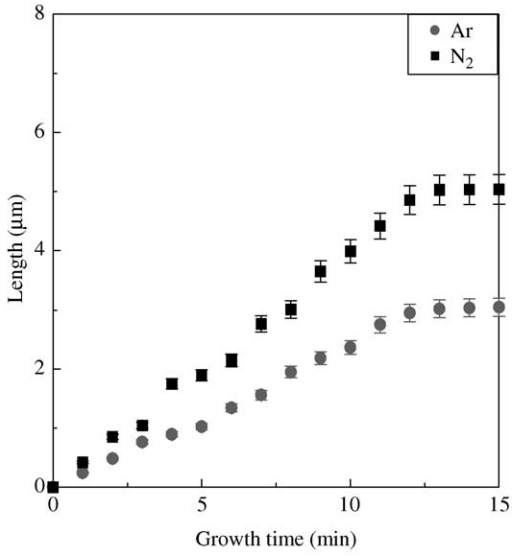

Figure 2 The nanowires length vs. growth time for ZnO nanowires grown in different carrier gases Ar and N_2.

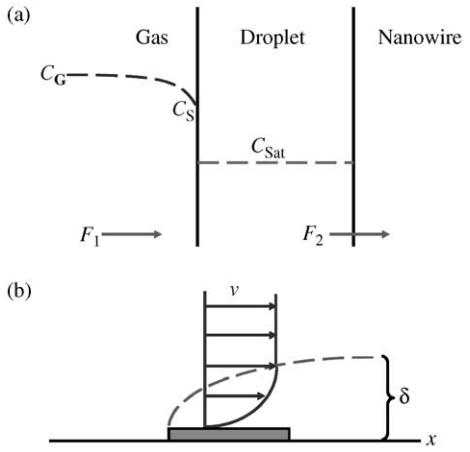

Figure 3 Schematic sketch of the chemical vapor deposition growth process for ZnO nanowires.

The deposition process of nanowires is a CVD process, which follows some fundamental steps: first, the reactants are transported to the droplet surface; followed by adsorption on the surface. As the droplet surface gets supersaturation with reactants, a chemical reaction takes place on the droplet-nanowire interface leading to the formation of the nanowire and reaction products. Afterwards, the reaction gas products are desorbed and transported away from the droplet surface. The process is schematically represented in Fig. 3 with the corresponding fluxes.

The gas phase flux (F_1) is given by the following relationship:

$$F_1 = h(C^* - C_{\mathrm{Sat}}) = \frac{D}{\delta}(C^* - C_{\mathrm{Sat}}) \tag{1}$$

where h is the gas-phase mass-transfer coefficient, C^* is the equilibrium concentration of the reactant, D is diffusivity of reactants in the bulk gas, C_{Sat} is saturating concentration of the reactants in the droplet, and δ is the thickness of the boundary layer (Fig. 3(b)), which can be expressed as:

$$\delta \propto \left(\frac{x^2\mu}{D\rho v}\right)^{1/2} \tag{2}$$

where μ is the viscosity of the bulk gas, ρ is the density of the bulk gas, and ν is the flow rate of the bulk gas. The rate of the reaction taking place at the droplet-nanowire interface is given by

$$F_2 = k_s C_{\mathrm{Sat}} \tag{3}$$

where k_s is the chemical reaction rate constant. Under the steady-state condition, we have

$$A_1 F_1 = A_2 F_2 \tag{4}$$

where A_1 is the adsorption area of the droplet and A_2 is the reaction area of the droplet-nanowire interface. On the basis of Equations 1, 3, and 4, we can obtain

$$C_{\mathrm{Sat}} = \frac{1}{1 + (A_2 k_s / A_1 h)} C^* \tag{5}$$

The growth rate R (μm/s) of the nanowire is

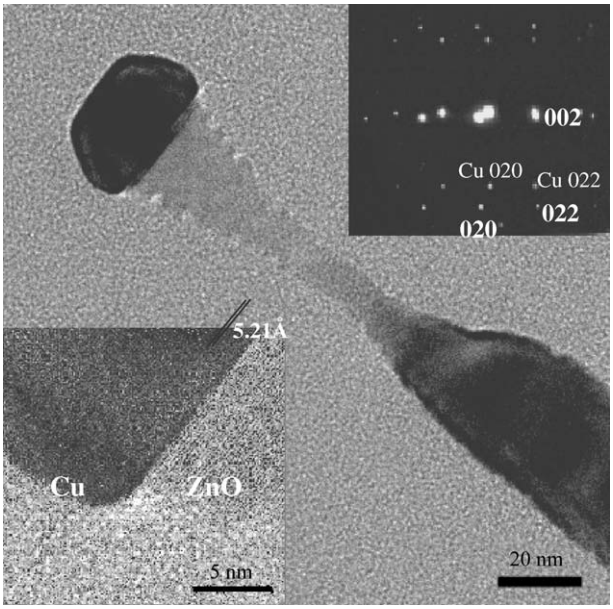

Figure 4 TEM image of the quenched ZnO nanowire. The corresponding electron diffraction pattern is shown in inset.

$$R = \frac{F_2}{N} \tag{6}$$

where N is the number of atoms incorporated into a unit volume of the nanowires. Equation 7 can be rewritten using Equations 5 and 6

$$R = \frac{F_2}{N} = \frac{k_s h}{h + (A_2/A_1)k_s} \frac{C^*}{N} \tag{7}$$

In the limiting cases, the growth rate is given by:

$$R = \frac{F_2}{N} = \frac{k_s C_{\mathrm{Sat}}}{N} \quad (H \gg k_s, \text{ reaction control}) \tag{8}$$

or

$$R = \frac{F_2}{N} = \frac{A_1}{A_2} h \frac{C^*}{N} = \frac{A_1}{A_2} \frac{D}{\delta} \frac{C^*}{N}$$
$$(H \ll k_s, \text{mass transfer control}) \tag{9}$$

The growth rate data shown in Fig. 2 can be explained with the use of Equations 7–9. If the growth of the nanowires is according to the reaction control (Equation 8), then the growth rate is governed by the values of k_s and C_{Sat}. However, k_s and C_{Sat} do not change with the time at the same temperature whether in the Ar or N_2 atmosphere. The viscosity of N_2 is smaller than that of Ar, hence the thickness of boundary layer is thinner in N_2 than in Ar. In this case, assuming the factors in Equation 9 except viscosity are independent of the atmosphere, the growth rate of nanowires would be faster in N_2 than in Ar on the basis of Equation 9, in which the growth rate is inversely proportional to the thickness of boundary layer. Therefore, we suggest that the growth of the nanowires be predominantly through mass transfer control, because the experiment results of the growth rate of the nanowires indicated in Fig. 2 is in good agreement with theoretical prediction expressed by Equation 9. Moreover, the ZnO nanowries fabricated in N_2 atmosphere grow faster in the longitudinal direction; that is, most of the reactants are consumed in longitudinal growth and the gas–solid condensation reaction in the sidewall of the nanowires is reduced. Therefore, the diameters of those ZnO

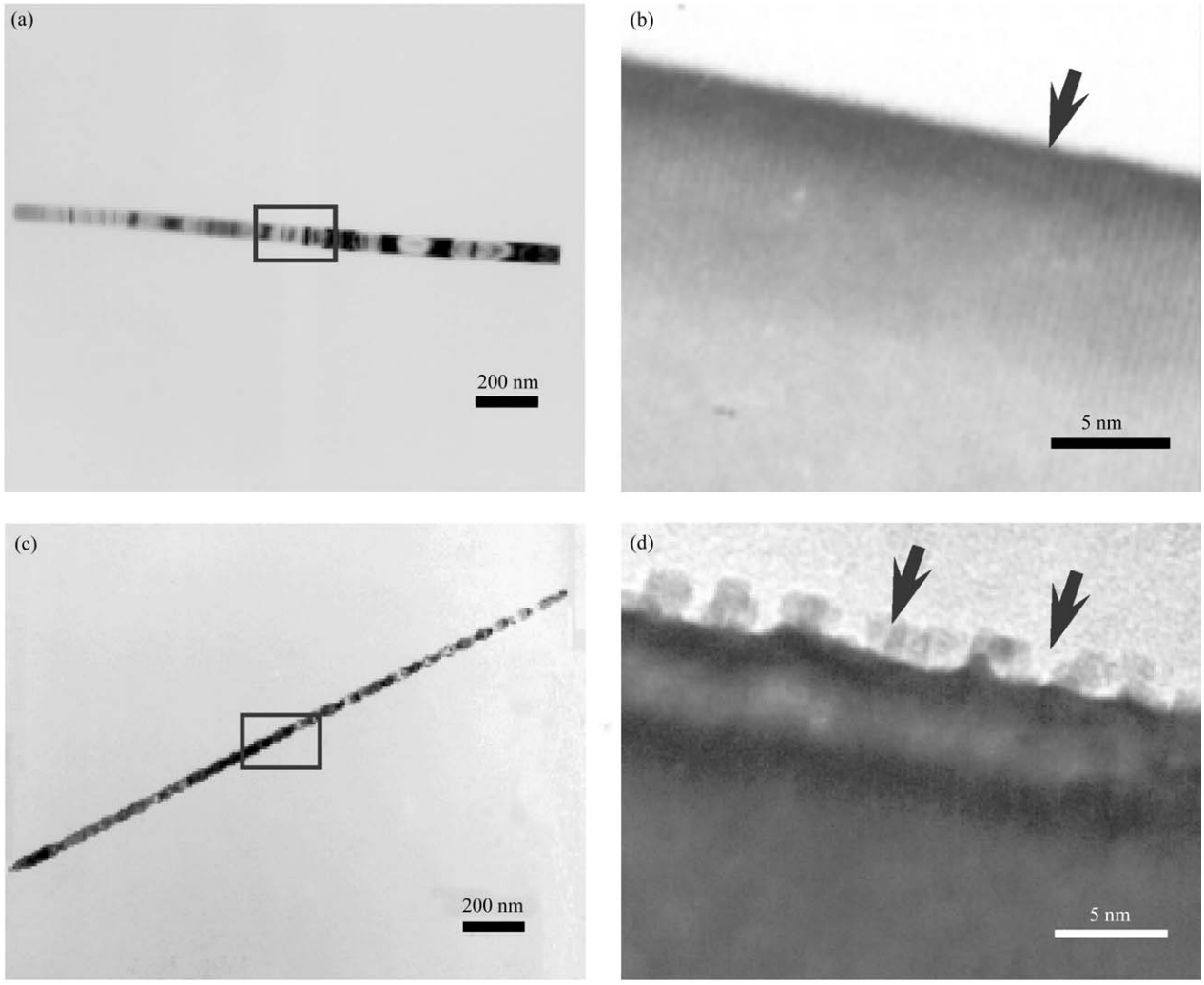

Figure 5 TEM bright view images and HRTEM images of the nanowires synthesized in Ar ((a) and (b)) and in N_2 ((c) and (d)).

nanowires fabricated in N_2 atmosphere are smaller than those fabricated in Ar atmosphere.

The HRTEM images and their corresponding selected area electron diffraction (SAED) pattern are shown in Fig. 4. The crystal with the thinner end appears in the HRTEM image of the tip of the ZnO nanowires quenched from high temperature. The possible mechanism of the nanowires growth is surface diffusion and such growth also depends on the precipitation rate. The slender region mentioned may be explained by the droplets being consumed during the nanowires growth. Progressive consumption of droplets during the growth leads to smaller diameters, and hence thinner nanowires. The distance between parallel lattice fringes as shown in Fig. 4 is about 5.21 Å, which is equal to the d-spacing of the [0 0 0 2] planes of ZnO nanowires. The SAED pattern (inset in Fig. 4) of the nanowires can be indexed to the reflection of hexagonal ZnO in (0 0 0 2) direction and includes Cu–Si–Zn alloy structure.

The ZnO nanowires synthesized in Ar and N_2 have a unique growth direction, i.e., [0 0 0 2], as evidenced by electron microscopy study. Examining the shape of the ZnO nanowires, we observe that the nanowires synthesized in the Ar (Fig. 5(a) and (b)) are straight with larger diameter and smooth morphology, while the surface morphology of those ZnO nanowires fabricated in N_2 (Fig. 5(c) and (d)) are quite different. These have smaller diameters and a periodic growth along the [0 0 0 2] with a screw-like shape. The difference between the ZnO nanowires synthesized in Ar atmosphere and those synthesized in N_2 atmosphere is believed to be caused by the variation of hydrodynamics. Two possible mechanisms contribute to the nanowire growth. The first is VLS growth mechanism. Second, the gas–solid condensation reaction in the sidewall of the nanowires affects the sidewall morphology of the nanowire. The growth of ZnO nanowires in Ar atmosphere is contributed by both of these two mechanisms and therefore those nanowires have the larger diameters and smooth sidewall surface, while the growth of nanowires in N_2 atmosphere is dominated by the VLS growth mechanism, leading to the formation of smaller diameter and screw-like nanowires.

The EDX spectrum (a) in Fig. 6 of the tip of nanowires shows that Cu and Si are the main constituents of the droplet, which catalyze the growth of ZnO nanowires. The spectrum (b) in Fig. 6 reveals that atomic weight percent of zinc (50.31%), oxygen (49.43%), and silicon (0.23%) constitute parts of the stem of the nanowires, and there is compositional uniformity along the growth direction. It is apparent that the Cu peak was generated by the copper grid. The impurity, such as C and Si also dissolved in to the ZnO nanowires. According to the Cu–Si phase diagram [10], it is proposed that the Cu thin film

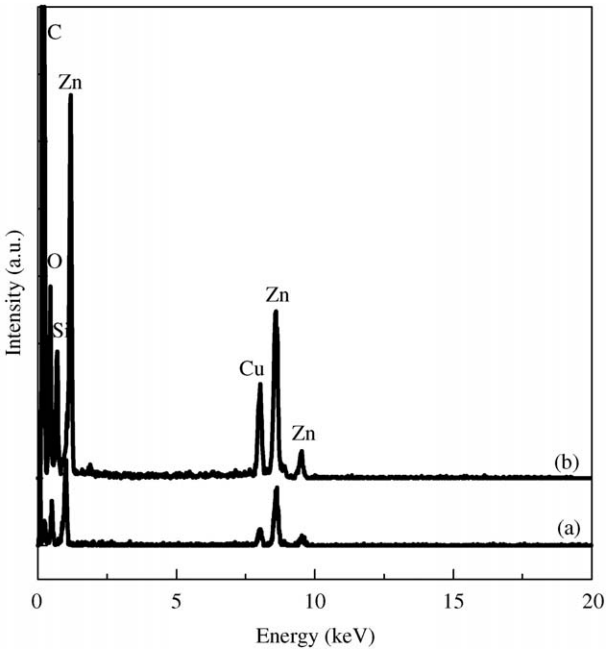

Figure 6 EDX spectra of (a) stem (b) tip of the nanowires grown with N_2.

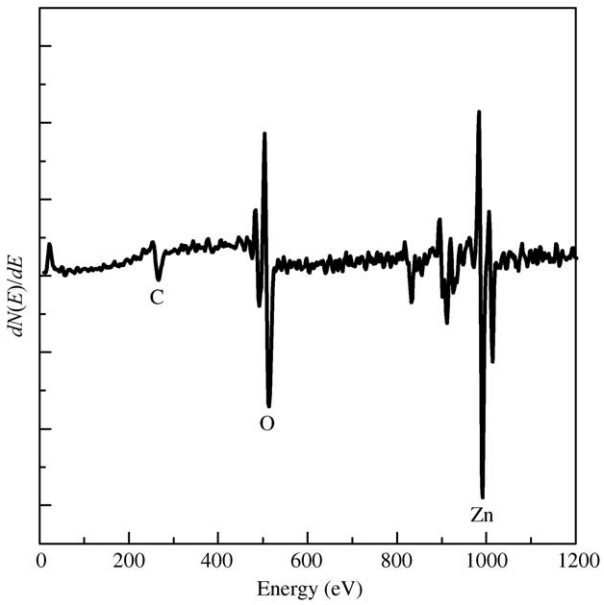

Figure 8 AES spectra of the ZnO nanowires synthesized in N_2.

reacted with the Si substrate and formed the Cu–Si alloy nanoparticles as the eutectic temperature of Cu and Si is lower than the synthesis temperature of the ZnO nanowires.

Fig. 7 is the XPS spectrum of the ZnO nanowires. The spectrum shows that there are Zn, O, Si, and C elements. The two strong peaks at 536.61 and 1026.00 eV, respectively, as shown in Fig. 7 agree with the O(1s) and Zn($2p^3$) binding energy for ZnO. The detection of small amounts of carbon can be attributed to the residual reactant adsorbed on the surface. We also observe the peak of Si as the ZnO nanowires were grown on the Si substrate.

The AES Spectrum of the ZnO nanowires in Fig. 8 indicates that the Auger peak corresponding to oxygen appears at 510 eV, and the peaks corresponding to zinc are at 833, 913, 991, 1013 eV, respectively. Weak peak of C is also observed at 273 eV as the carbon impurity in ZnO nanowires. With above EDX, XPS and AES examinations, the compositions of nanowires are found to be consistent with stoichiometric ZnO. The impurities such as C and Si dissolve in the nanowires but there is no nitrogen dissolved in it.

Fig. 9 shows the XRD pattern of the ZnO nanowires synthesized in Ar and N_2. Three diffraction peaks can be identified as $(1\,0\,0)$, $(0\,0\,2)$, and $(1\,1\,0)$ that correspond to the hexagonal ZnO, thereby confirming the crystalline phase of the ZnO nanowires with lattice constants $a = b = 3.25$ Å and $c = 5.20$ Å [11].

Optical properties of the ZnO nanowires were studied by photoluminescence (PL) spectroscopy at room temperature under 350 nm light excitation. Fig. 10 shows a strong ultraviolent (UV) emission at 380 nm

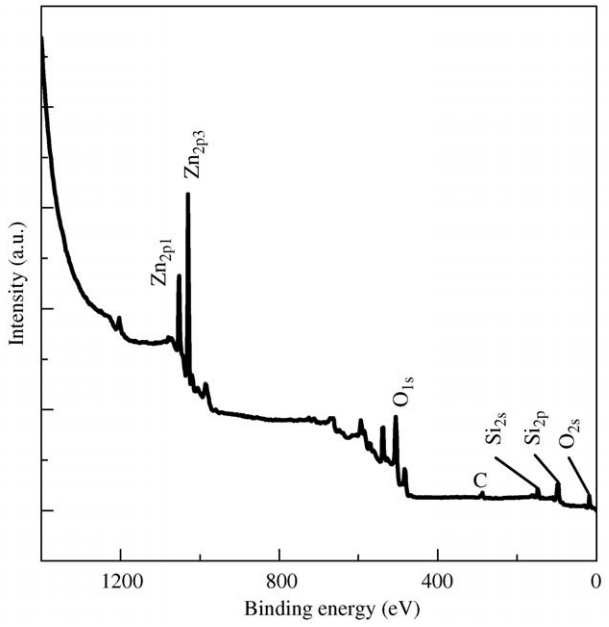

Figure 7 XPS spectra of the ZnO nanowires synthesized in N_2.

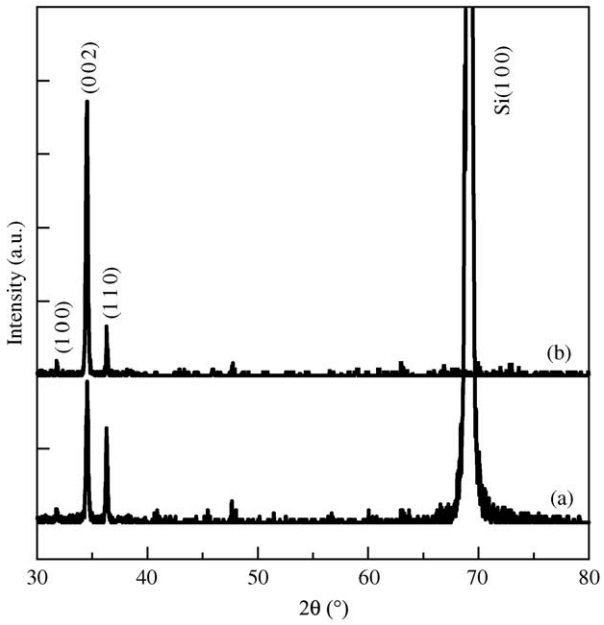

Figure 9 XRD patterns of ZnO nanowires synthesized in (a) Ar and (b) N_2.

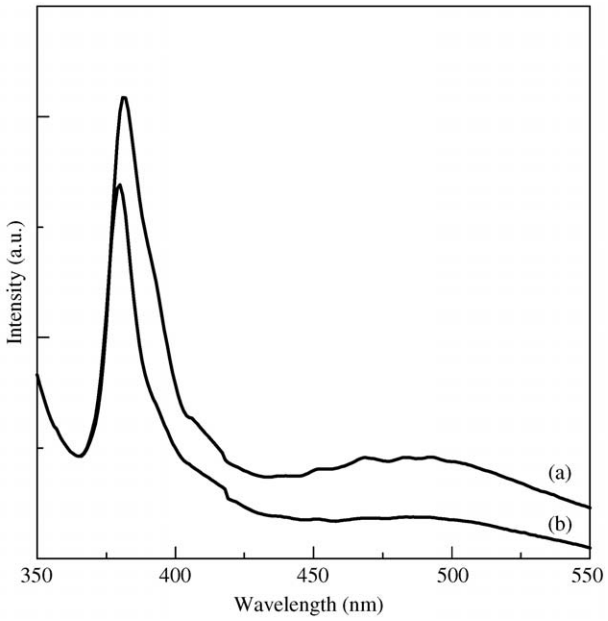

Figure 10 Photoluminescence spectra of ZnO nanowires grown in (a) N_2 and (b) Ar at room temperature.

can be observed. Curves (a) and (b) that correspond to the PL-spectra of ZnO nanowires synthesized in N_2 and Ar, respectively indicate that the ZnO nanowires synthesized in N_2 enhance the photoluminescence. The PL intensity caused by ZnO nanowires synthesized in N_2 is higher than those synthesized in Ar. It can be attributed this result to that the number density of the nanowires grown in N_2 is larger than those grown in Ar. An increase of the deep-level green light emission at ~ 520 nm for the nanowires fabricated in N_2 is also due to the increasing number density and larger surface area of the nanowires. In other words, the existence of N_2 enhances the growth of the ZnO nanowires and increases the photoluminescence of those nanowires.

4. Conclusions

In summary, the enhanced VLS growth ZnO nanowires in N_2 compared to in Ar was observed. Such enhancement is due to the lower viscosity of N_2 used in ZnO nanowires growth, which was supported by mass transfer control growth mechanism derived in the present study. The ZnO nanowires grown in different carrier gases, N_2 and Ar exhibits hexagonal structure with $\langle 0\,0\,0\,2 \rangle$ orientation. The photoluminescence analysis demonstrated that the nanowires grown in N_2 have stronger ultraviolet emission peak near at 380 nm in comparison with in Ar, which is attributed to larger number of density of nanowires grown in N_2.

Acknowledgment

This work was supported by the National Science Council of ROC under contrast number NSC 90-2212-E009-029.

References

1. M. H. HUANG, Y. WU, H. FEICK, N. TRAN, E. WEBER and P. YANG, *Adv. Mater.* **2** (2001) 113.
2. M. H. HUANG, S. MAO, H. FEICK, H. YAN, Y. WU, H. KIND, E. WEBER, R. RUSSO and P. YANG, *Science* **292** (2001) 1897.
3. Y. C. KONG, D. P. YU, B. ZHANG, W. FANG and S. Q. FENG, *Appl. Phys. Lett.* **78** (2001) 407.
4. L. D. ZHSNG, *Solid State Commun.* **115** (2000) 253.
5. S. Y. LI, C. Y. LEE and T. Y. TSENG, *J. Cryst. Growth* **247** (2003) 357.
6. A. M. MORALES and C. M. LEIBER, *Science* **279** (1998) 208.
7. Z. G. BAI, D. P. YU, H. Z. ZHANG, Y. DING, X. Z. GAI, Q. L. HANG, G. C. HIONG and S. Q. FENG, *Chem. Phys. Lett.* **303** (1999) 311.
8. T. THURN-ALBRECHT, J. SCHOTTER, G. A. KASTLE, N. EMLEY, T. SHIBUACHI, L. KRUSIN-ELBAUM, K. GUARINI, C. T. BLACK, M. T. TUOMINEN and T. P. RUSSELL, *Science* **290** (2000) 2126.
9. Y. KONDO and K. TAKAYANAGI, *ibid.* **289** (2000) 606.
10. Perry's Chemical Engineers' Handbook (McGraw-Hill, New York, 1984).
11. ICDD, International Center for Diffraction Data, JCPDS-ICDD, 2000.

Received 29 April 2003
and accepted 7 January 2004